Computational Condensed Matter 8 (2016) 14–21

Contents lists available at ScienceDirect

Computational Condensed Matter

journal homepage: http://ees.elsevier.com/cocom/default.asp

Theoretical study of structural stability, elastic, electronic and thermodynamic properties of $Sc_xGa_{1-x}P$ compounds by *ab initio* calculations

William Celin-Mancera [a], William López-Pérez [b], Álvaro González-García [b, *], Luz Ramírez-Montes [a, b], Rafael González-Hernández [b]

[a] Departamento de Ciencias Básicas, Universidad de la Costa, Barranquilla, Colombia
[b] Grupo de Investigación en Física Aplicada, Departamento de Física, Universidad del Norte, Barranquilla, Colombia

ARTICLE INFO

Article history:
Received 2 March 2016
Received in revised form
2 June 2016
Accepted 11 July 2016
Available online 16 July 2016

Keywords:
Structural and elastic stability
Electronic structure
Thermodynamic properties
DFT
GaP

ABSTRACT

We carried out a theoretical study on the structural stability, elastic, electronic and thermodynamic properties of the $Sc_xGa_{1-x}P$ compound ($x = 0, 0.25, 0.50, 0.75$ and 1) in the ZnS and NaCl crystallographic phases. For this purpose, we performed *ab initio* calculations using the DFT within LDA and GGA approximations. To solve the Kohn-Sham equations, we implemented the accurate full-potential linearized augmented plane wave method. From the results obtained, it can be noted that for the $0 \leq x \leq 0.30$ range, the most stable structure of $Sc_xGa_{1-x}P$ is the ZnS phase, and for the $0.30 < x \leq 1$ interval, the most stable structure is the NaCl phase. The structural results also show a phase transition from the ZnS to NaCl at a pressure of ~ 2.84 GPa for a Sc concentration value of 25%. Electronic band structure analysis shows that in the ZnS phase, for a 25% of Sc concentration, $Sc_xGa_{1-x}P$ is a direct semiconductor, and from 50% to 100% concentrations in the NaCl phase, the compound exhibits a metallic behavior. Calculated phase diagrams predict $Sc_xGa_{1-x}P$ to be stable as homogeneous alloy phases at high temperature for both ZnS and NaCl phases.

1. Introduction

The comprehensive study of new materials engineered from nitride compounds, and recently from phosphides, has enabled significant advances in the field of high-power and high-temperature electronics. Knowledge and characterization of these binary and ternary phosphide compounds remain scarce. Recently, motivation for the study and research of their properties has been triggered, due to their great importance in technological applications [1]. There are studies in the literature that describe the semiconductor behavior of binary phosphides [2]. Among them is gallium phosphide (GaP), which is an indirect semiconductor that crystallizes under normal conditions in the zinc sulphide (ZnS) structure ($F\overline{4}$ 3 m space group) with a lattice constant of 5.45 Å [2,3]. Moreover, it exhibits a structural phase transition into the sodium chloride (NaCl) structural phase ($Fm\overline{3}$ m space group) at a transition pressure whose experimental value is 26 GPa [4,5]. GaP has a band-gap energy of 2.35 eV [2,3], and its applications have enabled the manufacture of green light-emitting diodes (LEDs) [6,7]. Experimental studies have been reported that seek to improve the physical properties and luminescence of GaP in the manufacture of LED diodes by doping it with small concentrations of nitrogen [8]. With regard to scandium phosphide (ScP), there is little experimental research about its structural, electronic, and optical properties. Through X-ray studies, it is known that it crystallizes under normal conditions in the NaCl structural phase, with a lattice parameter of 5.31 Å at room temperature [9,10]. Theoretical studies on the structural and electronic properties of ScP predict that it has a metallic structure in the NaCl phase [11]. This same research reports that ScP could undergo a structural phase transition from the sodium chloride (NaCl) to the cesium chloride (CsCl) one at a transition pressure of 245.6 GPa [11]. Another theoretical study predicts that the ScP compound could crystallize in the CsCl phase, with a lattice constant of 3.33 Å, and also exhibits a metallic behavior in this structural phase [12].

The preference of GaP and ScP for either ZnS, NaCl or CsCl structure depends on the size ratio of their constituent ions. The

* Corresponding author.
E-mail address: alvarogonzalez@uninorte.edu.co (Á. González-García).

http://dx.doi.org/10.1016/j.cocom.2016.07.001

critical ratio of the cation to the anion that must satisfy ZnS, NaCl and CsCl structures are, respectively, 0.225, 0.414 and 0.732 [13]. On the other hand, for GaP semiconductor the ratio of Ga^{3+} radius (0.62 Å) to P^{3-} radius (2.12 Å) is 0.292. In addition, for ScP compound the ratio of Sc^{3+} radius (0.885 Å) to P^{3-} radius (2.12 Å) is 0.417. Therefore, as GaP radius ratio is closer to the ZnS one, will be more energetically favorable for GaP to fit in a ZnS structure rather than in a NaCl or CsCl one. On the contrary, for ScP will be more energetically favorable to fit in a NaCl structure rather than in a ZnS or CsCl one.

On the other hand, ternary transition-metal phosphides have received increased attention over the last few years, and new synthesis strategies have been developed [14]. As a result, there is now a large and constant growing list of ternary and higher-order transition-metal phosphides, showing very rich structural, chemical, and physical properties [15–17]. Thus, a precise knowledge of the structural and electronic properties and their compositional dependence in these semiconductor alloys is necessary in order to evaluate their expected range of applications. This has motivated recent studies on theoretical characterizations of $AlAs_{1-x}$ P_x, Ga_xIn_{1-x} P,Sc_xY_{1-x} P, In_{1-x} B_xP y Sc_{1-x} In_xP ternary alloys [18–22]. However, there is a ternary phosphides group, Sc_xGa_{1-x} P, that has not been yet studied neither theoretically nor experimentally. Therefore, in this paper we have studied the structural stability, phase transitions, elastic, electronic and thermodynamic properties of Sc_xGa_{1-x} P, through total energy first-principles calculations within the density functional theory framework.

2. Computational methods

This paper presents the study of the structural and electronic properties of Sc_xGa_{1-x} P in the NaCl (rocksalt), and ZnS (zinc-blende) phases through density functional theory (DFT) [23]. These phases were selected because binary compounds ScP and GaP crystallize at room temperature in NaCl and ZnS structures, respectively. The total energy calculations were performed by varying the scandium (Sc) concentrations in the ternary compound for $x = 0$, 0.25, 0.50, 0.75 and 1. The Kohn-Sham equations were solved by adopting the highly accurate full-potential linearized augmented plane-wave plus local orbitals (FP-LAPW + lo), as implemented in the WIEN2K numerical code [24]. The exchange-correlation effects were taken into account in the local density approximation (LDA) by Perdew and Wang parameterization [25], and the generalized gradient approximation (GGA) by Perdew-Burke-Ernzerhof (PBE) [26] Wu-Cohen (WC) [27] and Engel-Vosko (EV) [28] parameterizations. To achieve the convergence of the energy values, the wave functions in the interstitial region are expanded with a plane-wave cutoff up to a value of $K_{max} = 7.0/\text{Rmt}$, where Rmt is the smallest muffin-tin radius and K_{max} is the maximum length vector of the reciprocal lattice. The condition $G_{max} = 12\ \text{Ry}^{1/2}$ was used for the density and potential expansion in the interstitial region. We selected the values of 1.75, 1.95, and 1.65 *a.u* for Sc, Ga, and P atoms, respectively, as muffin-tin radius (Rmt). A mesh of 116 and 72 special *k*-points in the irreducible wedge of the Brilloiun zone was considered for binary compounds with ZnS and NaCl structures, respectively. For the Sc_xGa_{1-x} P ternary compounds, we used 32 and 24 *k*-points in the irreducible part of the Brillouin zone for the ZnS and NaCl phases, respectively. The electronic configurations of Sc, Ga, and P are [Ar] $3d^1$ $4s^2$, [Ar]$3d^{10}$ $4s^2$ $4p^1$, and [Ne]$3s^2$ $3p^3$, respectively. The structural parameters were obtained by fitting the total energy versus volume data to Murnaghan's equation of state [29]. Subsequently, by applying the WC and EV exchange-correlation potentials, electronic band structures were calculated using the equilibrium volume of Sc_xGa_{1-x} P in the NaCl and ZnS phases for each Sc concentration.

The disordered systems are represented by large supercells in which cations are replaced randomly. For the DFT calculations is not feasible to adequately reproduce the statistics of random alloys represented by such large supercells. With the special quasi-random structures (SQS), it is possible to adequately mimic the statistics of a random alloy in a relatively small supercell. They are ordered structures designed to reproduce the most important pair-correlation functions of a random alloy [30–33]. In Refs. [31–33], the authors were able to efficiently describe the random nature of the local cation environment and the distribution of vacancies by using the SQS scheme. Therefore, to model the Sc_xGa_{1-x} P compounds, we employed special quasi-random structures (SQSs) [30]. In this study, the Sc_xGa_{1-x} P compounds are modelled with ordered structures described in terms of periodically repeated supercells. SQS scheme allows us to select the simplest unit cell for each analyzed composition [30]. Fig. 1(a) shows the 8-atom tetragonal cell for the NaCl structure in a concentration value of $x = 0.25$; this cell was also used for concentration values of $x = 0.50$ and 0.75. This tetragonal cell is obtained by doubling the 4-atom tetragonal unit cell for NaCl. The 4-atom tetragonal unit cell for NaCl was obtained from a conventional NaCl cell. The tetragonal unit cell of NaCl has equal bases, but the lattice parameter is smaller than the lattice parameter of a conventional NaCl lattice, while the height corresponds to the lattice constant of a conventional NaCl. For this cell, the relationships are given by $a = a_0/2$, $c = a_0$ and therefore $c/a = 2$; where *a* corresponds to the side of the tetragonal unit cell base and *c* is the parameter along the z axis, as shown in Fig. 1 (a); a_0 is the lattice constant of a conventional NaCl cell. For the zincblende-like (ZnS) structures with concentrations $x = 0.25$, 0.50 and 0.75, the simplest structure is an eight-atom simple cubic structure centered on the faces with a lattice parameter $a = a_0$, as shown in Fig. 1(b); a_0 is the lattice constant of a conventional ZnS cell. In order to test the reliability of our results, 32-atom special quasirandom structures (SQS) were used to model Sc_xGa_{1-x} P compounds with $x = 0.25$, 0.50 and 0.75. These structures correspond to $2\times$ $2\times$ 1 tetragonal supercells for both NaCl and ZnS-like structures.

3. Results and discussion

3.1. Structural properties

Total energy versus volume data for the ZnS and NaCl phases of

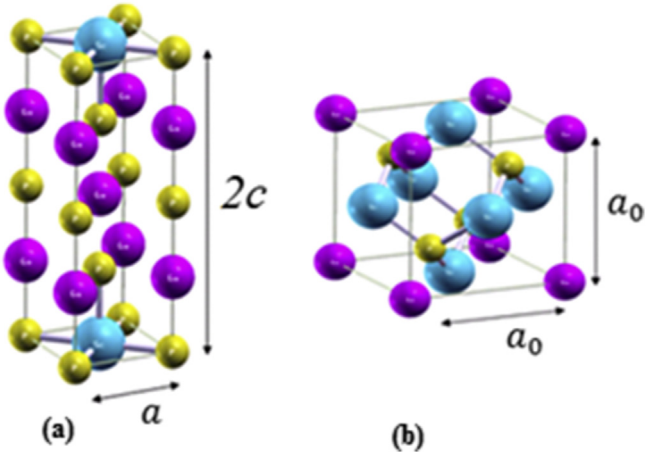

Fig. 1. Unit cell for Sc_xGa_{1-x} P for a concentration value of $x = 0.25$ on structures (a) NaCl and (b) ZnS. Blue, Purple and yellow atoms represent respectively Sc, Ga and P atoms. (For interpretation of the references to colour in this figure legend, the reader is referred to the web version of this article.)

Sc_xGa_{1-x} P are shown in Fig. 2. Energies and volumes are given per formula unit. The data are fit to Murnaghan's equation of state (EOS) for each phase. Fig. 2(a) shows the total energy curves as functions of the volume for a Sc concentration value of $x = 0.25$, corresponding to the WC potential. This figure shows that both structural phases are meta-stable, as there is a minimum in each curve, where the most stable structure is the ZnS phase. Fig. 2(b) also shows the total energy curves versus volume for a Sc concentration of $x = 0.50$ in the ternary compound, showing that the most stable structure is NaCl, which has the lowest energy. Fig. 2(c) shows that NaCl remains the most stable phase for a Sc concentration of $x = 0.75$. This behavior was also observed with the LDA and PBE potentials.

In order to study the structural stability of the Sc_xGa_{1-x} P compound, the transition pressure between ZnS and NaCl phases can be obtained from the common tangent of their energy-volume curves (Fig. 2). Because it is difficult to calculate accurate slopes, and hence to determine the most stable structure at finite pressure and temperature, we used the free energy G = E + PV − TS. Since our calculations do not include temperature effects, we neglect the last term and directly use the enthalpy H = E + PV. Fig. 3 shows the enthalpy-pressure curves for the $Sc_{0.25}$ $Ga_{0.75}$ P ternary compound, where the intersection points indicate the transition pressure value from the ZnS to NaCl structural phase. The obtained values were as follows: 5.03, 1.54, and 1.95 GPa in the LDA, PBE, and WC approximations, respectively. So far, there are no known reports of this transition pressure for the compound $Sc_{0.25}$ $Ga_{0.75}$ P. However, in order to check the consistency and accuracy of the procedure, we also calculated the transition pressure (from the ZnS to NaCl) of the GaP binary compound and obtained the value of pressure ~ 19.2 GPa, which is in good agreement with experimental and theoretical reports [34–36].

Table 1 shows the results of the structural parameters obtained for the different Sc concentrations in the NaCl and ZnS phases. These values correspond to the lattice constant $a(Å)$, equilibrium volume $V(Å^3)$, bulk modulus $B_o(GPa)$, and cohesion energy $E_{Coh}(eV)$ fit to Murnaghan's equation of state. The NaCl structural phase exhibits a relatively uniform increase of the lattice constant when the Sc concentration increases in the Sc_xGa_{1-x} P ternary compound, and hence in the equilibrium volumes. The lattice constants increase due to the fact that GaP host lattice receives Sc atoms slightly larger than Ga atoms. It can also be observed that the bulk modulus value decreases up to the concentration value 0.50 and increases slightly for the concentrations of 0.75 and 1. This trend could be due to the similarity of the lattice constants and bulk modulus values of the pure compounds GaP and ScP. On the other hand, the ZnS phase also exhibits a lattice constant increase, because the atomic radius of Sc (1.62 Å) is slightly larger than the atomic radius of Ga (1.41 Å) and P (1.28 Å). The cohesion energy becomes more negative with an increasing concentration of Sc, providing greater structural stability for the Sc_xGa_{1-x} P ternary compound.

Our results show that for ZnS (NaCl) structure of the Sc_xGa_{1-x} P compounds with PBE (LDA) functional, at concentrations of $x = 0.25$, 0.50 and 0.75, the cohesion energies per unit formula of 32-atom supercells are −7.50 eV (−8.93 eV),−8.17 eV (−10.00 eV) and −8.98 eV (−11.27 eV), respectively. Therefore, the total energy values are in the range from 1.0% to 1.2% lower than those of the 8-atom primitive cell at each concentration, as shown in Table 1. On the other hand, the calculated lattice constants for ZnS (NaCl) structure with PBE (LDA) potential, at concentrations of $x = 0.25$, 0.50 and 0.75, are ~ 0.018% (~ 0.19%) slightly higher than those of 8-atom primitive cell. Furthermore, the calculated bulk moduli for a 32-atom supercell with ZnS (NaCl) structure are ~ 0.9% (~ 0.39%) slightly lower than those of the 8-atom primitive cell. These results indicate that there are not significant differences between the values found for the cohesion energies per unit formula, lattice constants and moduli bulk of 32-atom supercells and those found for the 8-atom primitive cell of the Sc_xGa_{1-x} P ($x = 0.25$, 0.50 and 0.75) compounds with PBE (LDA) functional.

To analyze the results regarding the lattice parameter of the compound Sc_xGa_{1-x} P, Vegard's law was applied [37]. This law considers the atoms localized at the sites of an ideal lattice and assumes that the lattice constants are a linear function of the atomic concentration x. The equation that expresses this law is as follows:

$$a(Sc_xGa_{1-x}P) = xa_{ScP} + (1-x)a_{GaP}. \quad (1)$$

where a_{GaP} and a_{ScP} are the equilibrium lattice constants of the binary compounds and the term $a(Sc_xGa_{1-x}P)$ is the lattice constant of the ternary compound. Fig. 4 (a), (b) and (c) show the lattice constants as a function of the Sc concentration for the compound Sc_xGa_{1-x} P compared with the linear relationship of Vegard's law, showing deviations with respect to this law in the LDA, PBE, and WC approximations. The deviation parameter was determined through a quadratic fit by applying the following equation:

$$a(x) = xa_{ScP} + (1-x)a_{GaP} - \delta_a x(1-x). \quad (2)$$

In the NaCl phase, the deviation parameter δ_a of the ternary compound is as follows: $\delta_a = -0.113, -0.122$, and -0.099 with LDA, PBE, and WC, respectively. It was found that the value of the deviation parameter is relatively small, because the lattice constant values are close for the pure binary compounds. The LDA lattice constant of ScP is only 3.1% larger than the lattice constant for GaP in the NaCl structural phase; with the PBE and WC approximations, this difference is 3.2%. This low mismatch could produce the epitaxial growth of GaP/ScP semiconductor heterostructures. On the other hand, for the ZnS phase, the values of the deviation parameter were: $\delta_a = -0.194, -0.217$, and -0.184 with the LDA, PBE, and WC, respectively. In this case, the lattice constant of ScP is 7.3% larger than the lattice constant of GaP with the WC and LDA approximations; with the PBE, it is 7.2% larger. In addition, it can be noted that the lattice constant values corresponding to the NaCl structure are smaller than those for the ZnS structure, causing the

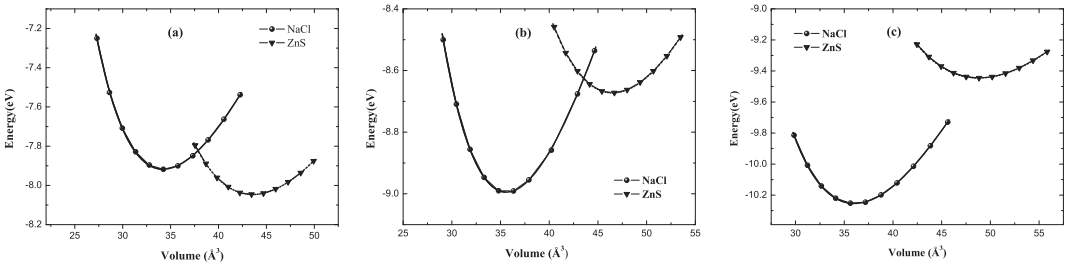

Fig. 2. Total Energy (eV) as a function of the volume (Å^3) for Sc_xGa_{1-x} P in the NaCl and ZnS phases at concentrations (a) $x = 0.25$, (b) $x = 0.50$ and (c) $x = 0.75$.

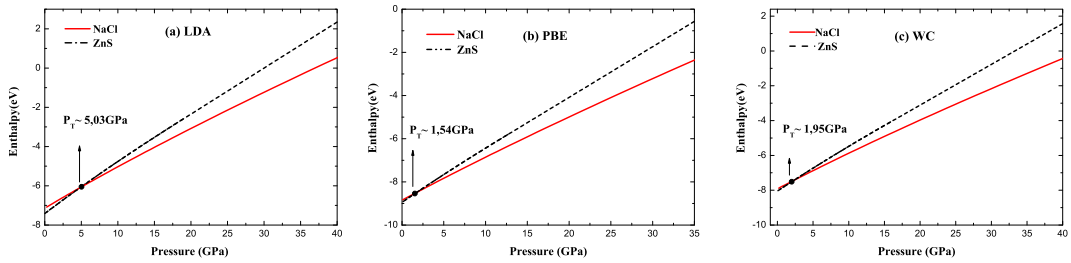

Fig. 3. Enthalpy as a function of pressure for $Sc_{0.25}$ $Ga_{0.75}$ P with the (a) LDA, (b) PBE and (c) WC approximations.

Table 1
Calculated structural properties of the ternary material Sc_xGa_{1-x} P in the NaCl and ZB structures with the LDA, PBE and WC potential. Experimental values are in parentheses. Energies and volumes are per unit cell. The parameter a corresponds to one side of the base in Fig. 1a and b. For the case of the rocksalt structure $a = a_0/2$, where a_0 is the lattice constant of a conventional NaCl cell.

		GaP		$Sc_{0.25}$ $Ga_{0.75}$ P		$Sc_{0.5}$ $Ga_{0.5}$ P		$Sc_{0.75}$ $Ga_{0.25}$ P		*ScP*	
		NaCl	*ZnS*	*NaCl*	*ZnS*	*NaCl*	*ZnS*	*NaCl*	*ZnS*	*NaCl*	*ZnS*
(*LDA*)	*a*(Å)	3.56	5.39	3.61	5.53	3.65	5.65	3.67	5.74	3.68	5.81
	$V(Å^3)$	32.31	39.21	33.28	42.24	34.60	45.26	34.96	47.49	35.23	49.14
	$E_{Coh}(eV)$	−7.88	−8.54	−8.84	−8.94	−9.89	−9.54	−11.14	−10.25	−12.45	−11.10
	$B_o(GPa)$	104.8	89.33	102.8	78.25	101.8	73.32	102.2	70.41	107.9	69.75
(*PBE*)	*a*(Å)	3.63	5.50	3.68	5.65	3.73	5.77	3.75	5.86	3.76	5.93
	$V(Å^3)$	34.29	41.75	35.49	45.19	36.88	48.17	37.32	50.53	37.62	52.22
	$E_{Coh}(eV)$	−6.11	−6.91	−7.13	−7.41	−8.24	−8.07	−9.50	−8.87	−10.83	−9.77
	$B_o(GPa)$	88.23	76.41	85.77	67.68	85.20	63.96	90.16	63.02	94.97	63.39
(*WC*)	*a*(Å)	3.59	5.44	3.63	5.58	3.68	5.70	3.70	5.80	3.71	5.87
	$V(Å^3)$	32.96	40.25	34.23	40.25	35.60	46.50	36.05	48.84	36.35	50.58
	$E_{Coh}(eV)$	−6.92	−7.59	−7.91	−8.07	−8.99	−8.67	−10.25	−9.44	−11.58	−10.33
	$B_o(GPa)$	96.3	84.43	95.7	74.33	93.3	69.55	97.1	66.73	101.4	66.67
(*Exp*)	*a*(Å)		*(5.45)*[a]							*(3.75)*[b]	
	$B_o(GPa)$		*(91.0)*[a]								

[a] Ref [2,3].
[b] Ref [9].

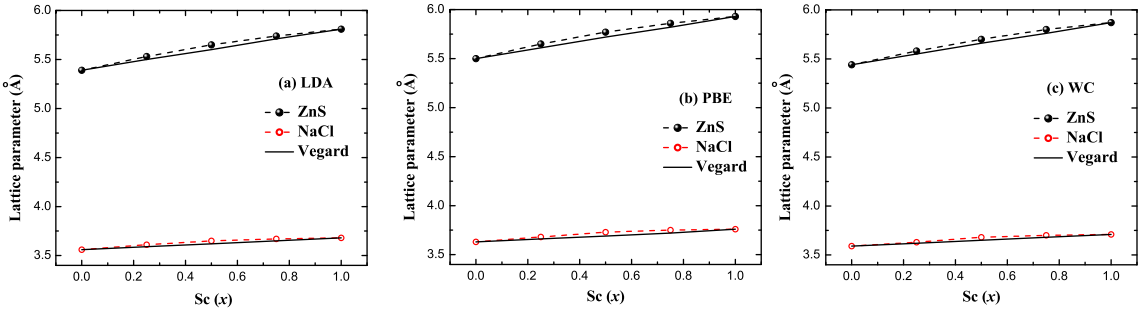

Fig. 4. Lattice constant (Å) as a function of Sc concentration for the compound Sc_xGa_{1-x} P in the NaCl and ZnS phases, with the (a) LDA, (b) PBE and (c) WC approximations. The calculations are compared to the linear fit of those values whose linear function corresponds to Vegard's law.

rigidity of the compound Sc_xGa_{1-x} P to be higher for the NaCl structure.

Fig. 5 shows the dependence of the minimum equilibrium energy on the Sc concentration for Sc_xGa_{1-x} P in the ZnS and NaCl phases, with the LDA, PBE, and WC approximations. The most stable structural phase is ZnS for Sc concentration in the $0 \leq x \leq 0.30$ range; however, it reverts to a NaCl structurally stable phase for concentration values of $0.30 < x \leq 1$. The transition concentration values correspond to $x = 0.304$, 0.404, and 0.325 in the LDA, PBE, and WC approximations, respectively. This structural transition point could be important for future applications of these new materials in experimental studies, and for exploring industrial applications.

3.2. Elastic properties

In order to further confirm the structure stability under strain, we calculated the elastic constants [38] of the Sc_xGa_{1-x} P compounds as a function of the Sc concentration, in the ZnS and NaCl structures, which are shown in Fig. 6. For the ZnS phase, there are three independent elastic constants, c_{11}, c_{12}, and c_{44} for a cubic structure. A stable cubic crystal should match with the conditions: $c_{44}>0$, $c>11|c_{12}|$, and $c_{11}+2c>120$ [39]. To validate our results, we found that the calculated GaP elastic constants (c_{11} = 125 GaP, $c_{12} = 52$ GPa, and $c_{44} = 64$ GPa) are in agreement with experimental reports ($c_{11} = 140$ GPa, $c_{12} = 62$ GPa, and $c_{44} = 70$ GPa) [40]. For the NaCl phase, there are six independent elastic constants, c_{11}, c_{12}, c_{13},

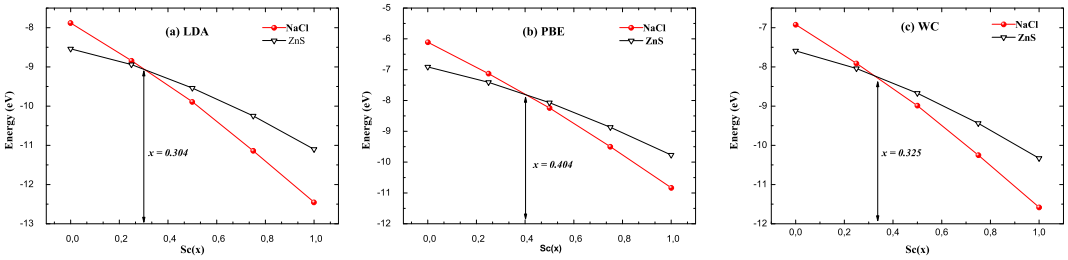

Fig. 5. Cohesion energy (eV per unit cell) as a function of Sc concentration for the compound $Sc_xGa_{1-x}P$ in the NaCl and ZnS phases with the (a) LDA, (b) PBE and (c) WC approximations.

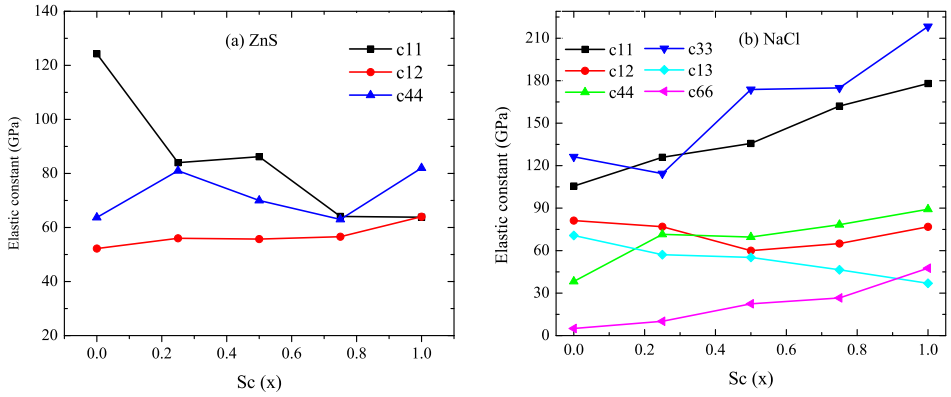

Fig. 6. Elastic constants as a function of Sc concentration for the compound $Sc_xGa_{1-x}P$ in the ZnS and NaCl phases with the PBE approximation.

c_{33}, c_{44}, and c_{66} for a tetragonal structure. A stable tetragonal crystal should match with the conditions: $c_{33}>0$, $c_{44}>0$, $c_{66}>0$, $c_{11}>|c_{12}|$, $c_{11}+c_{12}>0$, and $c_{11}+c_{33}-c_{13}>0$ [41]. In the ZnS phase, the Ga–P atoms form a covalent bond that is stronger than the Sc–P bond, which appears to be a metallic bond. For this reason, the cohesive energy and bulk modulus are greater in GaP than those in $Sc_xGa_{1-x}P$. Therefore, it is expected a decreasing in the c_{11} coefficient with the increase of *Sc* concentration, as it is observed in Fig. 6. In addition, c_{44} coefficients increased slightly from 0 to 0.25 of *Sc* concentration, however the system is still elastically stable at the ZnS phase. From the elastic stability criterion, we observed that $Sc_xGa_{1-x}P$ ($0\leq x\leq 1$) compounds in the ZnS and NaCl phases are all mechanically stable. However, the ZnS phase is unstable for the ScP compound at 0 GPa, since its elastic constants do not satisfy the mechanical stability criteria of cubic structure. In general, for the $Sc_xGa_{1-x}P$ alloy, our calculated values of the independent elastic constants lie in the range of corresponding to GaP and ScP binary compounds, as shown in Fig. 6.

3.3. Electronic properties

The electronic properties of the $Sc_xGa_{1-x}P$ ternary compound were examined for the ZnS and NaCl crystallization phases. It was found that the ZnS crystalline phase of the ternary compound exhibits a semiconductor behavior, while the NaCl phase exhibits a metallic behavior. For the ZnS structural phase, the electronic properties were calculated using the Engel-Vosko (EV) approximation, which gives a better energy band splitting by improving the exchange potential at the expense of less agreement in the exchange energy [28]. The results show that the GaP band-gap is 2.32 eV, which is closer to the experimental value 2.35 eV [2] as compared to PBE approximation (1.44 eV).

Fig. 7 shows the electronic band structure for $Sc_xGa_{1-x}P$ (32-atom SQS cells) for concentrations of (a) $x = 0.25$, (b) 0.50, (c) 0.75, and (d) $x = 1$, all of them in the ZnS phase. The Fermi level E_F is set to zero energy. For concentration values of $x = 0.25$, 0.50, 0.75 and 1, all four structures exhibit a direct band-gap of ~ 1.57 eV, ~ 1.59 eV, ~ 1.84 eV and ~ 2.00 eV, respectively, at $\Gamma-\Gamma(x = 0.25, 0.50$ and $0.75)$ and $X-X$ ($x = 1$) points, which is of great importance for potential applications in LEDs manufacturing. It is important to highlight that ScP is a *X*-direct semiconductor for the zinc blende structure. This semiconductor nature of ScP is different from those found for ScP in NaCl and CsCl phases, which exhibit a metallic behavior. Our results for ScP in the zinc blende phase are in agreement with previously reported data [12].

3.4. Thermodynamic properties

In order to study the thermodynamic stability of $Sc_xGa_{1-x}P$ compound, we calculated the phase diagram based on the regular-solution model [42] using 32-atom SQS supercells for the rock-salt and zincblende-like structures. The Gibbs free energy of mixing for the $Sc_xGa_{1-x}P$ compound is expressed by the following expression:

$$\Delta G_m = \Delta H_m - T\Delta S_m, \tag{3}$$

where ΔH_m and ΔS_m are the enthalpy and entropy of mixing respectively. *T* is the absolute temperature. The mixing enthalpy of $Sc_xGa_{1-x}P$ compound can be obtained from the calculated total energies by the expression

$$\Delta H_m = E_{tot}^{Sc_xGa_{1-x}P} - xE_{tot}^{ScP} - (1-x)E_{tot}^{GaP}. \tag{4}$$

The mixing enthalpy ΔH_m can also be expressed as

$$\Delta H_m = \Omega(x)x(1-x), \tag{5}$$

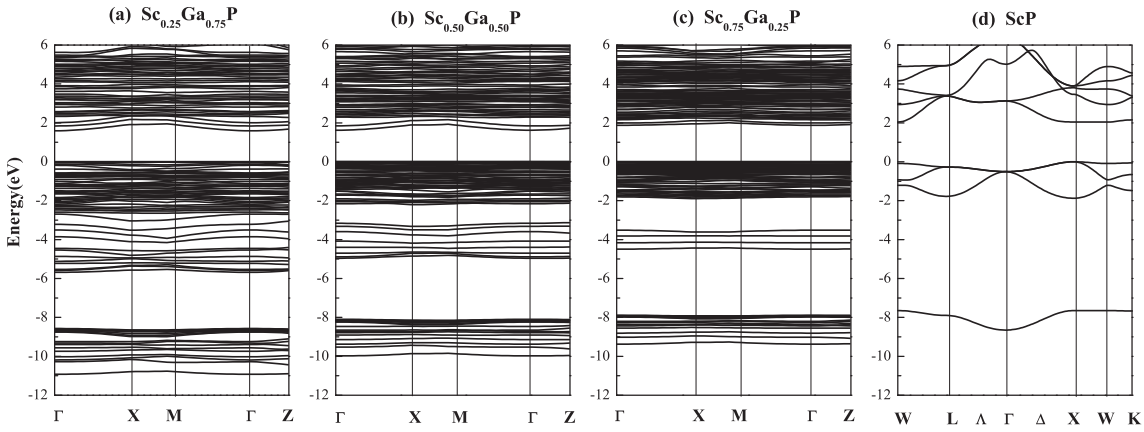

Fig. 7. Energy band structures for Sc_xGa_{1-x} P (32-atom SQS cells) for concentrations of (a) $x = 0.25$, (b) 0.50, (c) 0.75, and (d) $x = 1$, all of them in the ZnS phase within the EV approximation. The Fermi level E_F is set to zero energy.

where $\Omega(x)$ is the interaction parameter which depends on the material. Using Eqs. (4) and (5), we have calculated $\Omega(x)$ values (per cation-anion pair) at different compositions. The x-dependent interaction parameter is obtained from a linear fit to the $\Omega(x)$ values. The linear fit gives $\Omega(x)$=0.4118x+0.8608 eV/pair and $\Omega(x)$=−0.0204x+1.0146 eV/pair for ZnS-LDA and NaCl-LDA, respectively. The average values of the x-dependent Ω in the range $0 \leq x \leq 1$ calculated from these equations are 1.0667 eV/pair and 1.0044 eV/pair, respectively. We observe a larger interaction parameter Ω for ZnS than that of the NaCl phase. Therefore, we expect a higher mixing enthalpy in the zincblende-type structure. Using linear x-dependent and average values of the interaction parameter $\Omega(x)$, we draw the formation enthalpies of the Sc_xGa_{1-x} P compounds for both ZnS and NaCl with LDA functional. The average values of the x-independent interaction parameters $\Omega(x)$ are used to draw ΔH_m for both rock-salt and zinc-blende structures, as shown in Fig. 8(a) by the dotted and solid curves, respectively. Additionally, we draw ΔH_m using the linear x-dependent Ω, as shown in Fig. 8(b). Using the average values of the x-independent Ω it was found that the mixing enthalpies were positive for both NaCl and ZnS structures. As we predicted, the mixing enthalpy for ZnS is higher than that of NaCl structure, as shown in Fig. 8(a). It was also found, through the x-dependent interaction parameter, that the mixing enthalpy for a given concentration differs depending on structures. The mixing enthalpies for both ZnS and NaCl Sc_xGa_{1-x} P compounds are all positive (see Fig. 8(b)) indicating that the system has tendency to segregate in their constituents at normal growth temperatures. The mixing enthalpy of ZnS Sc_xGa_{1-x} P compounds is less positive than that obtained for NaCl Sc_xGa_{1-x} P at $0<x<0.35$ concentration range. This result indicates that the ZnS structure is more stable than the NaCl phase at that concentration range. In the $0.35<x\leq 1$ concentration the rock-salt phase is more stable than the zinc-blende phase. Recent first-principles and experimental thermodynamics studies of IIIB doped-IIIA-V systems have also found a phase transition at intermediate and high IIIB dopant concentration [43–45]. Recently, Zukauskaite et al. found a phase transition from wurtzite ($B4$) to cubic ($B1$) crystal structures for Y_xAl_{1-x} N at $x = 0.75$ by ab-initio calculations [43].

The mixing entropy ΔS_m is defined as

$$\Delta S_m = -R[x\ln x + (1-x)\ln(1-x)], \tag{6}$$

where R is the perfect gas constant. Using Eqs. (3)–(6), we calculate T-x-dependent ΔG_m, it used to construct the T-x phase diagram which predicts stable, metastable, and unstable mixing zones of Sc_xGa_{1-x} P compounds. The critical temperature occurs at a point where both the first and second derivatives of the free energy are zero, i.e., there is no curvature. At a temperature lower than the critical alloy mixing-demixing temperature T_c, the two binodal points are determined as those points at which the common tangent line touches the ΔG_m curves. The two spinodal points are determined as those points at which the second derivative of ΔG_m is zero. The resulting phase diagrams of Sc_xGa_{1-x} P compounds for

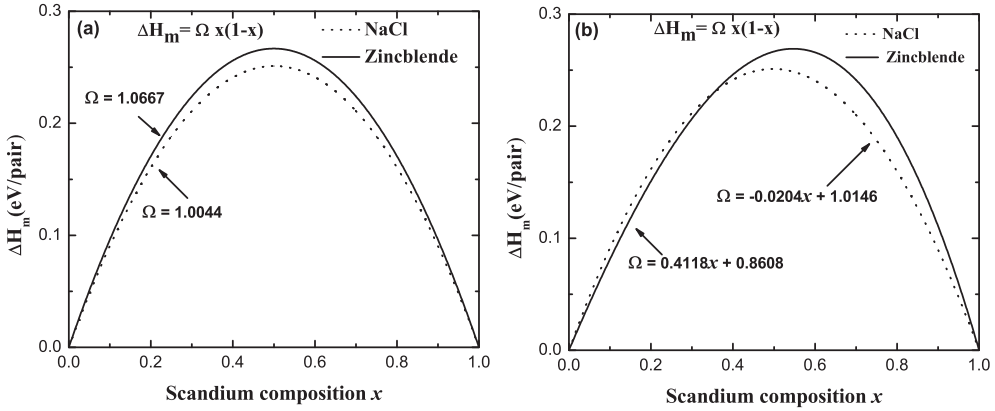

Fig. 8. Mixing enthalpy ΔH_m per cation-anion pair as a function of scandium concentration for the Sc_xGa_{1-x} P compound. Solid and dotted curves indicate ΔH_m for both ZnS-LDA and NaCl-LDA structures, respectively, with the (a) x-independent and (b) x-dependent interaction parameters Ω.

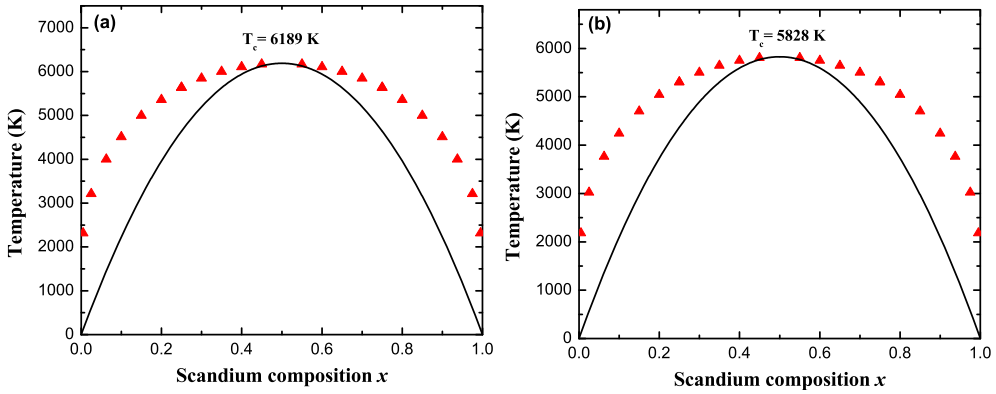

Fig. 9. (a) ZnS-LDA and (b) NaCl-LDA phase diagram as a function of scandium concentration for the $Sc_xGa_{1-x}P$ compound. Solid line indicate *T*-*x*-dependent spinodal curve and red triangles line is the *T*-*x*-dependent binodal curve. (For interpretation of the references to colour in this figure legend, the reader is referred to the web version of this article.)

ZnS and NaCl structures with *x*-independent Ω are plotted in Fig. 9 (a) and (b), respectively. We have calculated the phase diagram using the average values of *x*-dependent Ω, hence the phase diagram looks symmetric.

In the zinc-blende phase for scandium concentration of 0.25 (Fig. 9 (a)), a stable compound is observed at a temperature of 6000 K. At a temperature of 5000 K, the compound shows a metastable phase, and at a temperature of 3000 K the compound is unstable. The compound with $x = 0.5$ is unstable at these temperatures, however it is stable above 6189 K. The compound with $x = 0.75$ shows a similar behavior to that of the compound with $x = 0.25$ at these temperatures. In the NaCl phase, a similar behavior is observed, with the difference that the compound with $x = 0.5$ is stable at the temperature of 6000 K. The melting temperature of GaP is 1730 K [40], whereas the melting point of ScP is greater than 2280 K [46]. On the binodal curves, two stable phases coexist, whereas in the metastable phase region the phase segregation through nucleation and growth is presented. Inside the spinodal curves, the mixture of two phases of GaP and ScP is unstable. Outside the binodal curves, single-phase $Sc_xGa_{1-x}P$ is stable. In addition, we observe a higher critical alloy mixing-demixing temperature for ZnS (Tc=6189 K) than that of the NaCl phase (Tc=5828 K). This is due to a higher mixing enthalpy in the zinc-blende type structure. The spinodal curve in the phase diagram indicates the *T*-dependent equilibrium solubility limit, i.e., the miscibility gap. For temperatures and compositions above this curve a homogeneous alloy is predicted. The wide range between spinodal and binodal curves indicates that this alloy may exist as a metastable phase. In Fig. 9, we can see that $Sc_xGa_{1-x}P$ compounds are unstable over a wide range of intermediate compositions at room temperature. From our phase diagram, more stable alloys are likely to form at high temperature. Given that the mixing entropic contribution to the free energy difference is always negative, and ΔH_m is positive in our results, the effect of temperature will be very important at high values (Eq. (3)). At high temperatures the entropic term stabilizes the alloy. Our results indicate that the $Sc_xGa_{1-x}P$ compounds are stable at high temperatures. As we predicted, the large enthalpy value of $Sc_xGa_{1-x}P$ compounds suggests a large value of Ω, and consequently a high critical temperature.

4. Conclusions

Structural, elastic and electronic properties of the $Sc_xGa_{1-x}P$ compounds in the ZnS and NaCl structural phases were studied by applying the LDA, PBE, and WC approximations, within the density functional theory framework. The results show that the lattice parameters of the $Sc_xGa_{1-x}P$ compound increase with the Sc concentration, showing a small deviation from Vegard's law. The structural results also show a structural phase transition from the ZnS to NaCl phase at a pressure of ~ 2.84 GPa for a Sc concentration value of 25%, but there are no experimental reports for comparison. Regarding the electronic properties, $Sc_xGa_{1-x}P$ ($x = 0.25$) ternary compound presents a direct band gap of 1.57 eV at Γ point, which is of great importance for potential applications in LEDs manufacturing. It was found, with the *x*-independent interaction parameter, that the mixing enthalpies were positive for both NaCl and ZnS structures ($0 \leq x \leq 1$). The mixing is more favorable in NaCl structures over the entire Sc-composition range. It was also found, through the *x*-dependent interaction parameter, that the mixing enthalpy for a given concentration differs depending on structures, and on the interaction between atoms of constituents. With the *x*-dependent interaction parameter, it has been found that the ZnS structure is the most stable phase at $0 \leq x < 0.35$ concentration range. In the $0.35 < x \leq 1$ concentration range, the rock-salt phase is more stable than the zinc blende phase. Calculated phase diagrams predict that the $Sc_xGa_{1-x}P$ alloys to be stable at high temperature for both ZnS and NaCl phases. In the absence of experimental results, it is expected that our structural, electronic and thermodynamics calculations can be used not only to cover the lack of data but also to open the possibility for further investigations for the $Sc_xGa_{1-x}P$ compounds.

Acknowledgements

This work has been carried out with the financial support of Universidad del Norte and Colciencias (Administrative Department of Science, Technology and Research of Colombia) under "Convocatoria 658 – Convocatoria para proyectos de investigación en ciencias básicas año 2014".

References

[1] M.M. Ferhat, A. Zaoui, M. Certier, H. Aourag, Phys. B 252 (1998) 229.
[2] R. Ahmed, F. Aleem, S.J. Hashemifarb, H. Akbarzadehb, Phys. B 403 (2008) 1876.
[3] R.W.G. Wyckoff, Crystal Structures, second ed., Krieger, Malabar, 1986.
[4] R.J. Nelmes, M.I. McMahon, S.A. Belmonte, Phys. Rev. Lett. 79 (1997) 3668.
[5] O. Arbouche, B. Belgoumene, B. Soudini, Y. Azzaz, H. Bendaoud, K. Amara, Comput. Mater. Sci. 47 (2010) 685.
[6] L. Lin, G.T. Woods, T. Callcott, Phys. Rev. B 63 (2001) 235107.
[7] R.Z. Bachrach, W.B. Joyce, R.W. Dixon, J. Appl. Phys. 44 (1973) 5458.
[8] J. Chamings, S. Ahmed, S.J. Sweeney, V.A. Odnoblyudov, C.W. Tu, Appl. Phys. Lett. 92 (2008) 021101.
[9] C. Hazell, Acta Cryst. 16 (1963) 71.

[10] W.M. Yim, E.J. Stofko, R.T. Smith, J. Appl. Phys. 43 (1972) 254.
[11] A. Maachou, B. Amranib, M. Driz, Phys. B 388 (2007) 384.
[12] A. Tebboune, D. Rached, A. Benzair, N. Sekkal, A.H. Belbachir, Phys. Status Solidi (b) 243 (2006) 2788.
[13] N.W. Ashcroft, N.D. Mermin, Solid State Physics, Thomson Learning, Inc., 1976.
[14] A.E. Henkes, Y. Vasquez, R.E. Schaak, J. Am. Chem. Soc. 129 (2007) 1896.
[15] D.N. Talwar, Phys. E 20 (2004) 321.
[16] M. Othman, E. Kasap, N. Korozlu, J. Alloys Compd. 496 (2010) 226.
[17] G. Guisbiers, M. Wautelet, L. Buchaillot, Phys. Rev. B 79 (2009) 155426.
[18] F. Annane, H. Meradji, S. Ghemid, F. El Haj-Hassan, Comput. Mater. Sci. 50 (2010) 274.
[19] A.R. Degheidy, S.A.A. Elwakil, E.B. Elkenany, J. Alloys Compd. 574 (2013) 580.
[20] W. Lopez-Perez, P. castro-Diago, L. Ramirez-Montes, A. Gonzalez-Garcia, R. Gonzalez-Hernandez, Pilosophical Mag. 96 (2016) 498.
[21] A. Gonzalez-Garcia, W. Lopez-Perez, R. Palacio-Mozo, R. Gonzalez-Hernandez, Comput. Mater. Sci. 91 (2014) 279.
[22] W. López-Pérez, Nicolás Simon-Olivera, J. Molina-Coronell, A. González-García, R. González-Hernández, J. Alloy Compd. 574 (2013) 124.
[23] P. Hohenberg, W. Kohn, Phys. Rev. 136 (1964) 864. W. Kohn and L. J. Sham. Phys. Rev. 140 (1965) 1133.
[24] P. Blaha, K. Schwarz, G.K.H. Madsen, D. Kvasnicka, J. Luitz, WIEN2k an Augmented Plane Wave+Local Orbitals Program for Calculating Crystal Properties, Techn.UniversitatViena, Austria, 2001.
[25] J.P. Perdew, Y. Wang, Phys. Rev. B 45 (1992) 13244.
[26] J.P. Perdew, K. Burke, M. Erzerhot, Phys. Rev. Lett. 77 (1996) 3865.
[27] Z. Wu, R.E. Cohen, Phys. Rev. B 73 (2006) 235116.
[28] E. Engel, S.H. Vosko, Phys. Rev. B 47 (1993) 13164.
[29] F.D. Murnaghan, Proc. Natl. Acad. Sci. U. S. A. 30 (1994) 244.
[30] A. Zunger, S.H. Wei, L.G. Ferreira, J.E. Bernard, Phys. Rev. Lett. 65 (1990) 353.
[31] H. Wang, A. Chroneos, C. Jiang, U. Schwingenschlogl, Special quasirandom structures for gadolinia-doped ceria and related materials, Phys. Chem. Chem. Phys. 14 (2012) 11737.
[32] A. Chroneos, C. Jiang, R.W. Grimes, U. Schwingenschlogl, H. Bracht, E centers in ternary Si1-x-yGexSny random alloys, Appl. Phys. Lett. 95 (2009) 112101.
[33] Jeremy W. Nicklasa, John W. Wilkins, Accurate ab initio predictions of III-V direct-indirect band gap crossovers, Appl. Phys. Lett. 97 (2010) 091902.
[34] M. Causa, R. Dovesi, C. Roetti, Phys. Rev. B 43 (1991) 11937.
[35] M. Baublitz, A.L. Ruoff, J. Appl. Phys. 53 (1982) 6179.
[36] L. Li, W. Jian-Jun, W. Xue-Min, L. Hui-Na, W. Wei-Dong, Chin. Phys. B 20 (2011) 06201.
[37] L. Vegard, Z. Phys. 5 (1921) 17.
[38] A.H. Reshak, M. Jamal, J. Alloys Compd. 543 (2012) 147.
[39] B.B. Karki, G.J. Ackland, J. Crain, J. Phys. Condens. Matter 9 (1997) 8579.
[40] S. Adachi, Properties of Semiconductor Alloys: Group-IV, III-V and II-VI Semiconductors, Wiley, Chichester, 2009.
[41] D.C. Wallace, Thermodynamics of Crystals, Wiley, New York, 1972.
[42] R.A. Swalin, Thermodynamics of Solids, Wiley, New York, 1961.
[43] A. Zukauskaite, C. Tholander, J. Palisaitis, P.O.A. Persson, V. Darakchieva, N.B. Sedrine, F. Tasnadi, B. Alling, J. Birch, L. Hultman, J. Phys. D. Appl. Phys. 45 (2012) 422001.
[44] C. Hoglund, J. Birch, B. Alling, J. Bareno, Z. Czigany, P.O.A. Persson, G. Wingqvist, A. Zukauskaite, L. Hultman, J. Appl. Phys. 107 (2010) 123515.
[45] C. Hoglund, J. Bareno, J. Birch, B. Alling, Z. Czigany, L. Hultman, J. Appl. Phys. 105 (2009) 113517.
[46] L.N. Komissarova, A.A. Menkov, L.M. Vasileva, Inorg. Mater 1 (1965) 1361.